Modeling of Active Stability Control on KSTAR and NSTX

Oksana Katsuro-Hopkins[1], S.A. Sabbagh[1], J.M. Bialek[1],
H.K. Park[2], J.Y. Kim[3], K.-I. You[3], A.H. Glasser[4], L.L. Lao[5]

[1]Department of Applied Physics, Columbia University, New York, NY, USA

[2]Pohang University of Science and Technology, Korea

[3]National Fusion Research Institute, Daejeon, Korea

[4]Los Alamos National Laboratory, Los Alamos, NM, USA

[5]General Atomics, San Diego, CA, USA

NSTX Physics Meeting

January 14, 2008

PPPL, Princeton, NJ

Numerical design study to optimize advanced stability of KSTAR merging present experimental results & machine design

- Motivation
  - Design optimal global MHD stabilization system for KSTAR with application to future burning plasma devices

- Outline
  - Free boundary equilibrium calculations
  - Ideal stability operational space for experimental profiles
  - RWM stability and VALEN-3D modeling
  - Advanced feedback control algorithm and performance

Korea Superconducting Tokamak Advanced Research will study steady-state advanced tokamak operation & technology

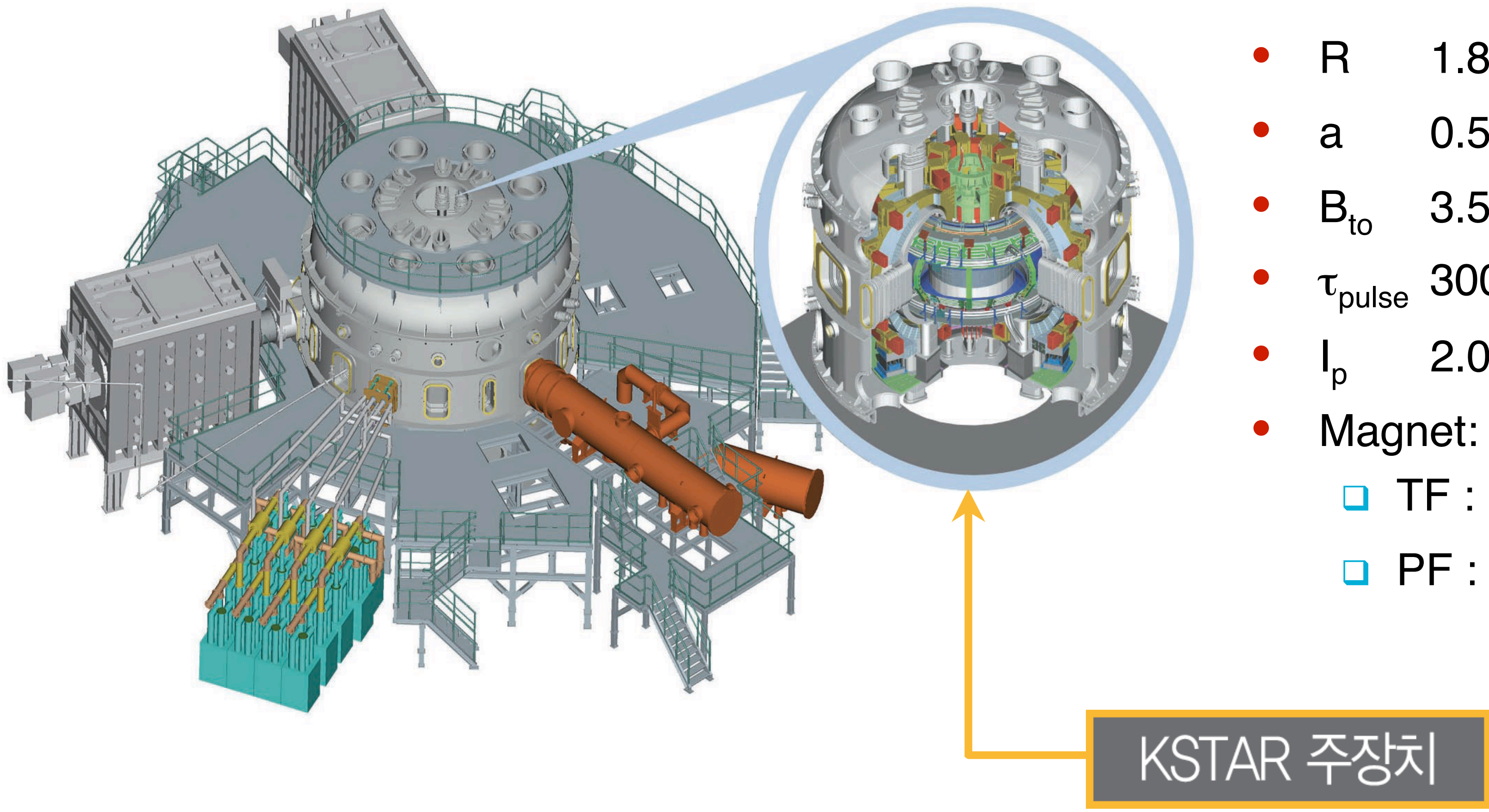

Parameters:

- R 1.8m
- a 0.5 m
- B_{to} 3.5 T
- τ_{pulse} 300 s
- I_p 2.0 MA
- Magnet:
  - TF : Nb3Sn,
  - PF : NbTi

KSTAR configuration used in EFIT calculations

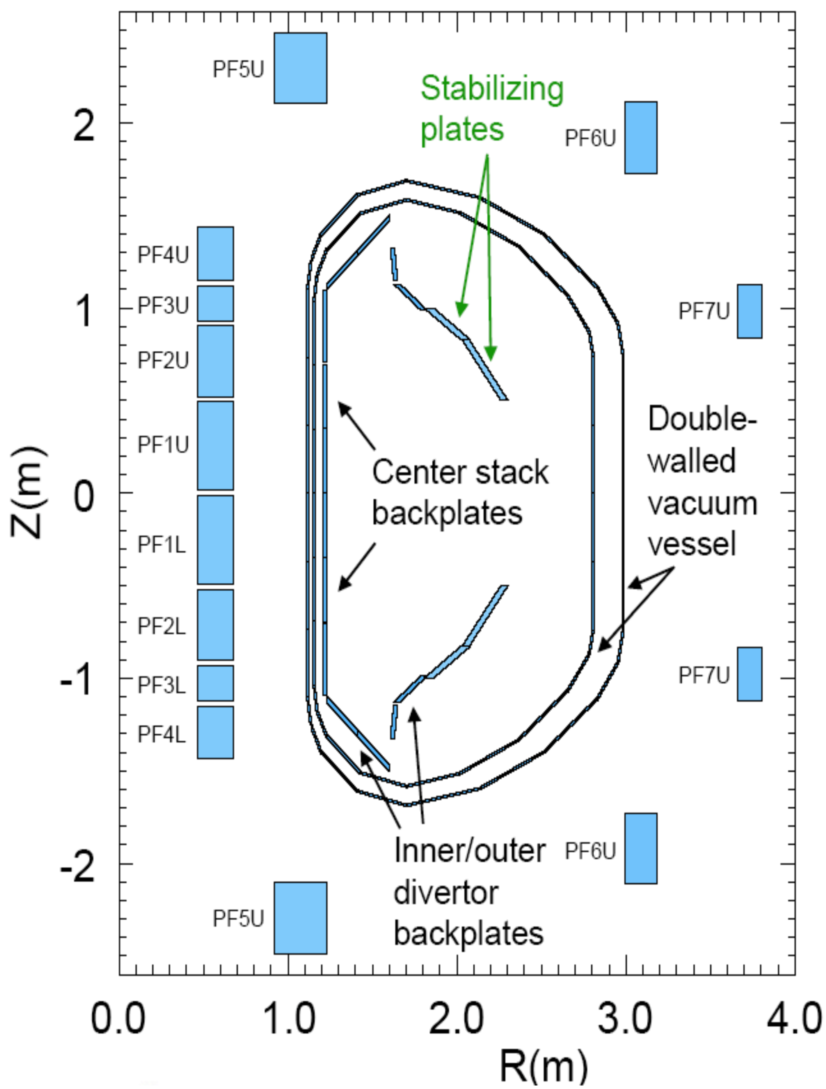

- EFIT industry-standard tool
  - Free-boundary equilibria
  - Expandable range of equilibria
- Data from KSTAR design drawings
- Passive stabilizers/vacuum vessel included.
  - Important for start up studies
  - Reconstructions during events that change edge current (e.g. ELMs)

Equilibrium variations produced to scan (l_i,β_n)

- Boundary shape
  - Free-boundary equilibria with high shaping κ~2,δ~0.8
  - Shaping coil currents constrained to machine limits
- Pressure profile
  - Generic "L-mode", edge p'=0
  - H-mode, modeled from DIII-D
- q profile
  - Monotonic to mild shear reversal with $q_0>1$ and $(q_0-q_{min})<1$
- Variations in (l_i,β_n) produced
  - $0.5 \le l_i \le 1.2;\ 0.5 \le \beta_n \le 8.0$

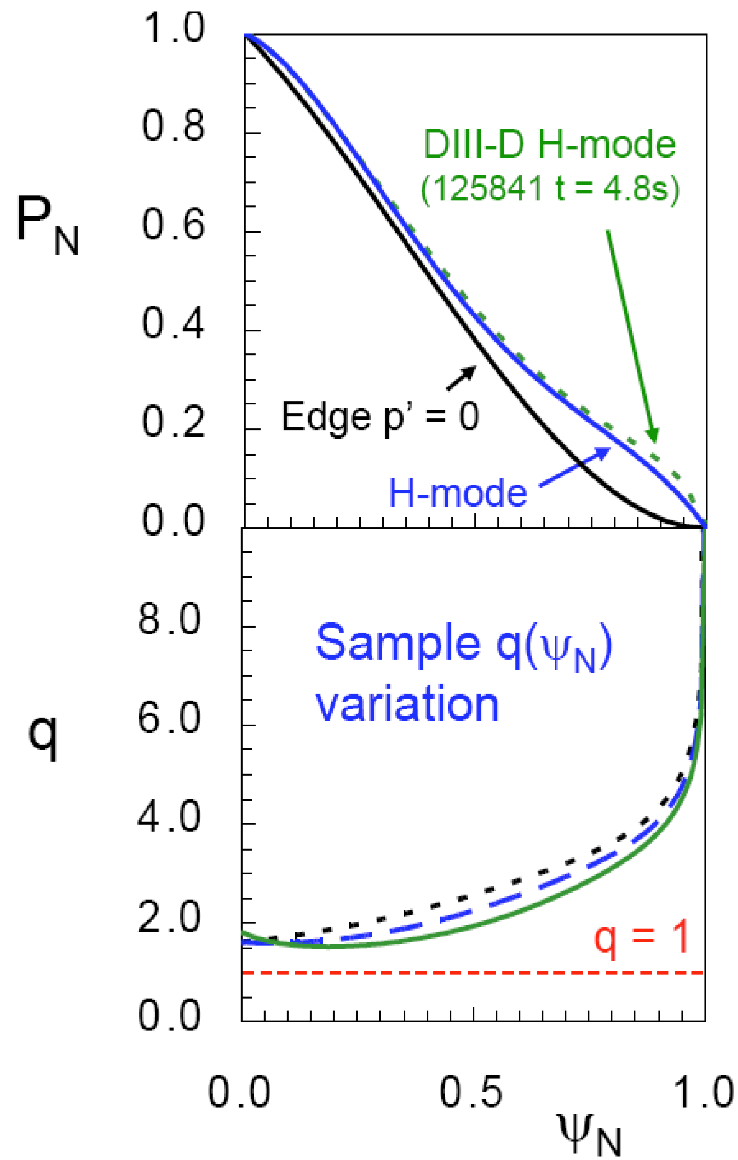

Ideal stability(DCON): conducting wall allows significant passive stabilization for n=1 H-mode pressure profile

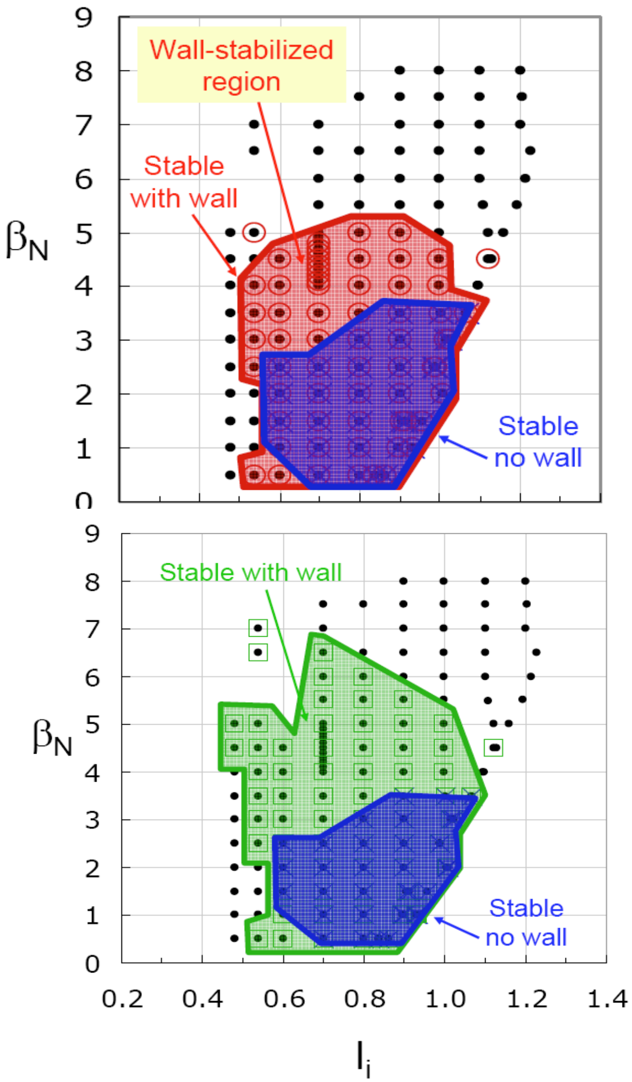

- "inner" wall used

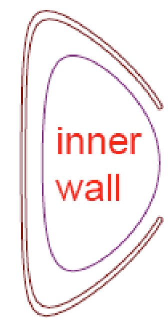

- Wall-Stabilized β_n is a factor of two greater then for equilibrium without wall at $l_i \sim 0.7$
- Wall-Stabilized β_n from DCON agrees with VALEN-3D value

- "outer" wall used

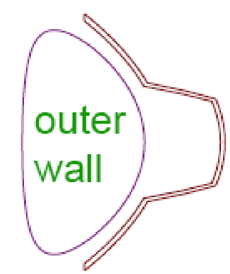

- Wall-Stabilized $\beta_n > 6.5$ (larger than the result using "inner" wall at $l_i \sim 0.7$)
- Optimistic, but does not agree with VALEN-3D. "Inner" wall is more realistic and should be used in DCON analysis

L-mode pressure profile has large n=1 stabilized region

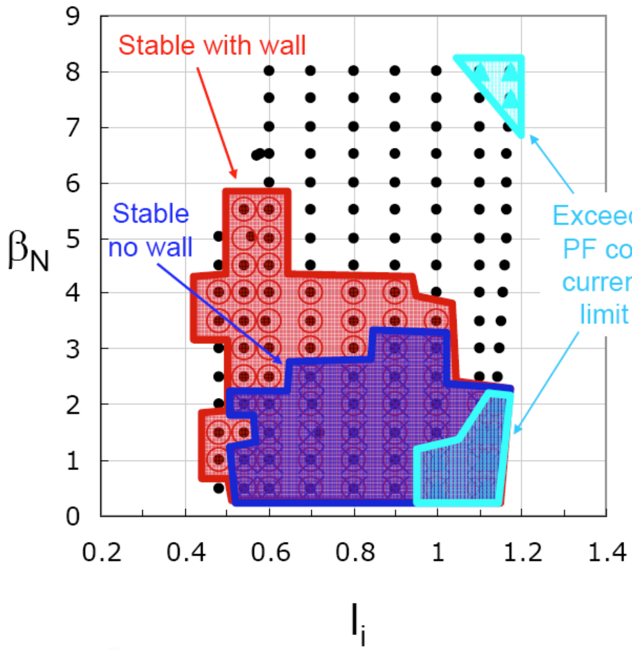

- "inner" wall used
- Wall-Stabilized region at lowest l_i (Unfavorable for n=0 stabilization)
- Possible difficulty to access with L-mode confinement.

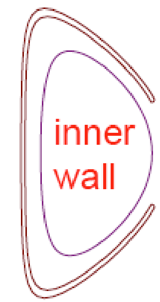

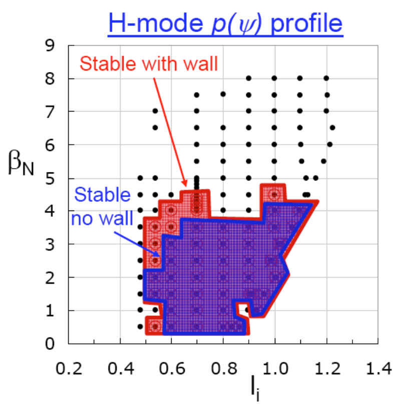

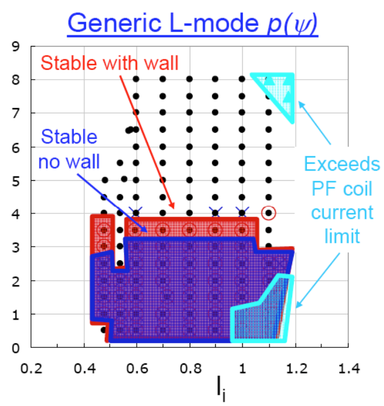

- **n=2 stability** has higher no-wall & lower with-wall limits than n=1 for H-mode and L-mode pressure profile
  - Internal n=2 modes were observed in NSTX during n=1 active RWM stabilization.

Conducting hardware, IVCC set up in VALEN-3D*
based on engineering drawings

n=1 RWM passive stabilization currents

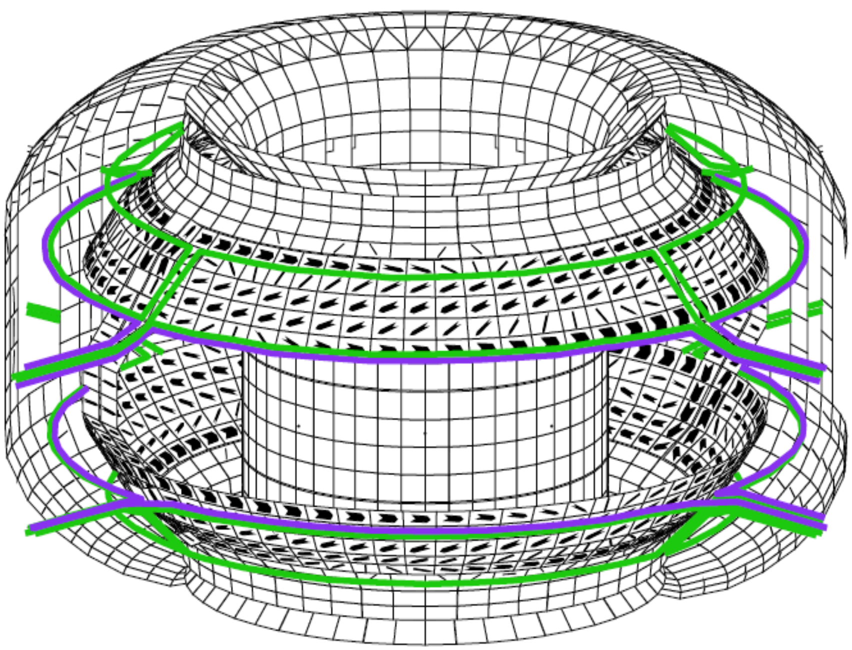

IVCC (RWM) control coils
(upper,middle,lower)

*Bialek J. et al 2001 Phys. Plasmas **8** 2170

- Conducting structures modeled
  - Vacuum vessel with actual port structure
  - Center stack back-plates
  - Inner and outer divertor back-plates
  - Passive stabilizer
  - PS Current bridge
- Stabilization currents dominant in PS
  - 40 times less resistive than nearby conductors.

VALEN 3-D code reproduces n=1 DCON β_n ideal wall limit

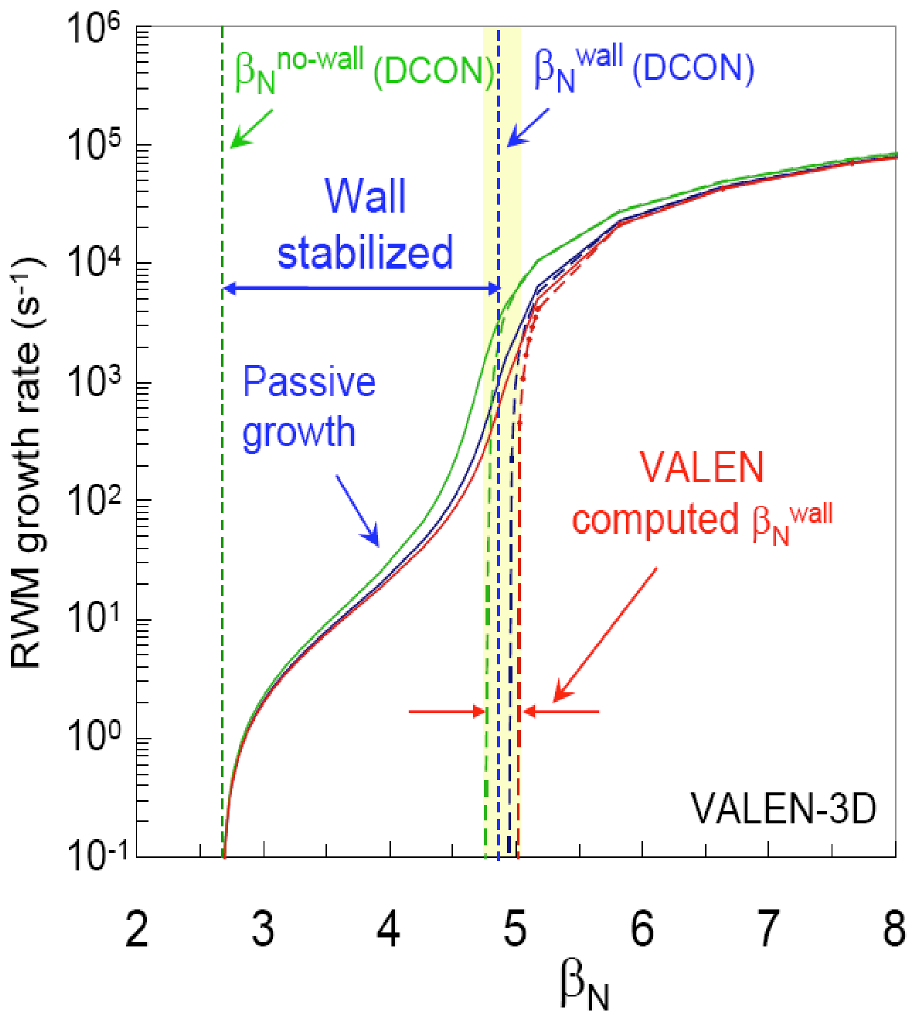

- Important cross-check VALEN-3D/DCON calibration
- Equilibrium β_n scan with l_i=0.7 H-mode pressure profile
- DCON n=1 β_n limits:
  - $\beta_n^{no\text{-}wall} = 2.6$
  - $\beta_n^{wall} = 4.8$
- VALEN-3D n = 1 β_n^{wall}
  - $4.77 < \beta_n^{wall} < 5.0$
  - Range generated by various RWM eigenfunctions from equilibria near $\beta_n = 5.$

IVCC allows active n=1 RWM stabilization near ideal wall.

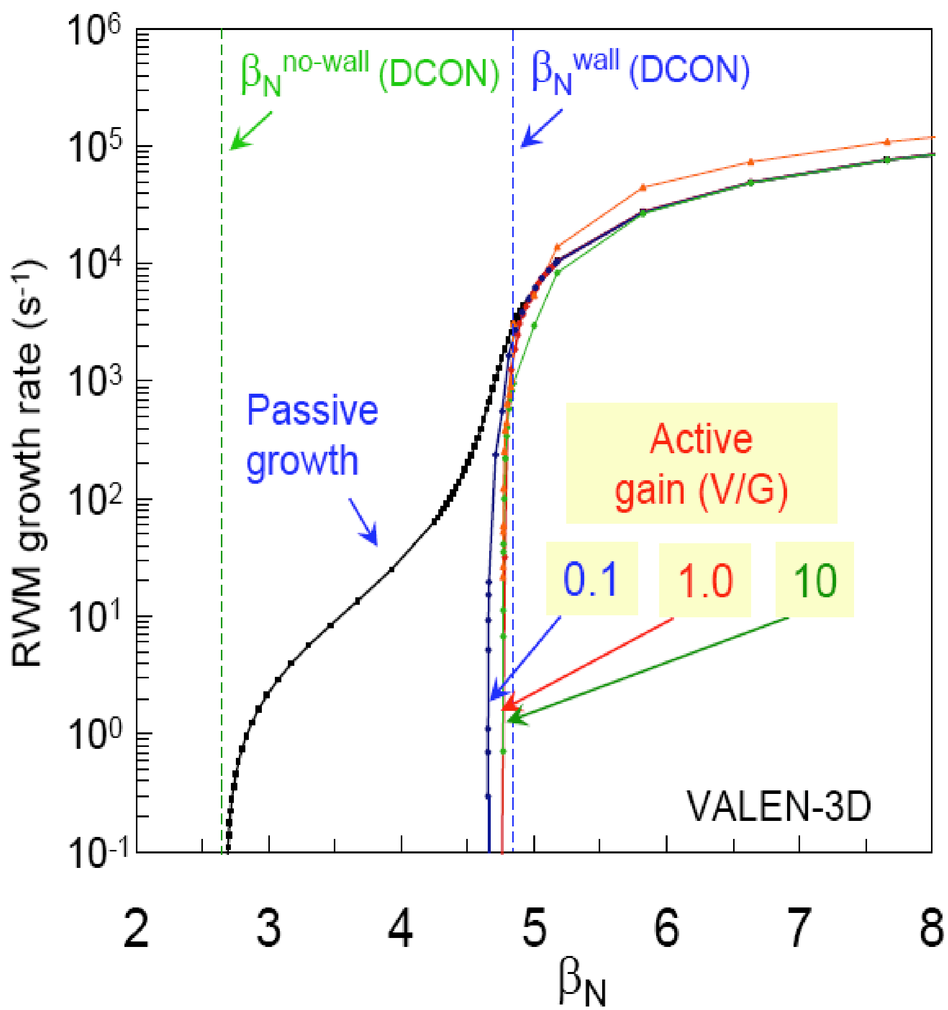

- Active n=1 RWM stabilization capability with

$$C_\beta = \frac{\beta_n - \beta_n^{no\ wall}}{\beta_n^{wall} - \beta_n^{no\ wall}} > 98\%$$

  - Optimal ability for mode stabilization
  - Mid-plane IVCC used
- Equilibrium β_n scan with l_i=0.7 H-mode pressure profile
- Computed β_n limits
  - $\beta_n^{no-wall}$ = 2.56
  - β_n^{wall} = 4.76

Noise on RWM sensors sets control system power

- Gaussian white noise
  - ~1.5Gauss RMS, based on noise in DIII-D RWM B_p sensors
  - Minimum estimate of control power consumption
    - Perfect response to RWM
    - No other coherent modes

- Experimental sensor input
  - NSTX B_p sensor during RWM active stabilization
  - Maximum estimate of control system power consumption
    - DC offset from resonant field amplification; stray field from passive plate currents
    - The $\Delta B/B_0$ larger in ST than at higher apsect ratio

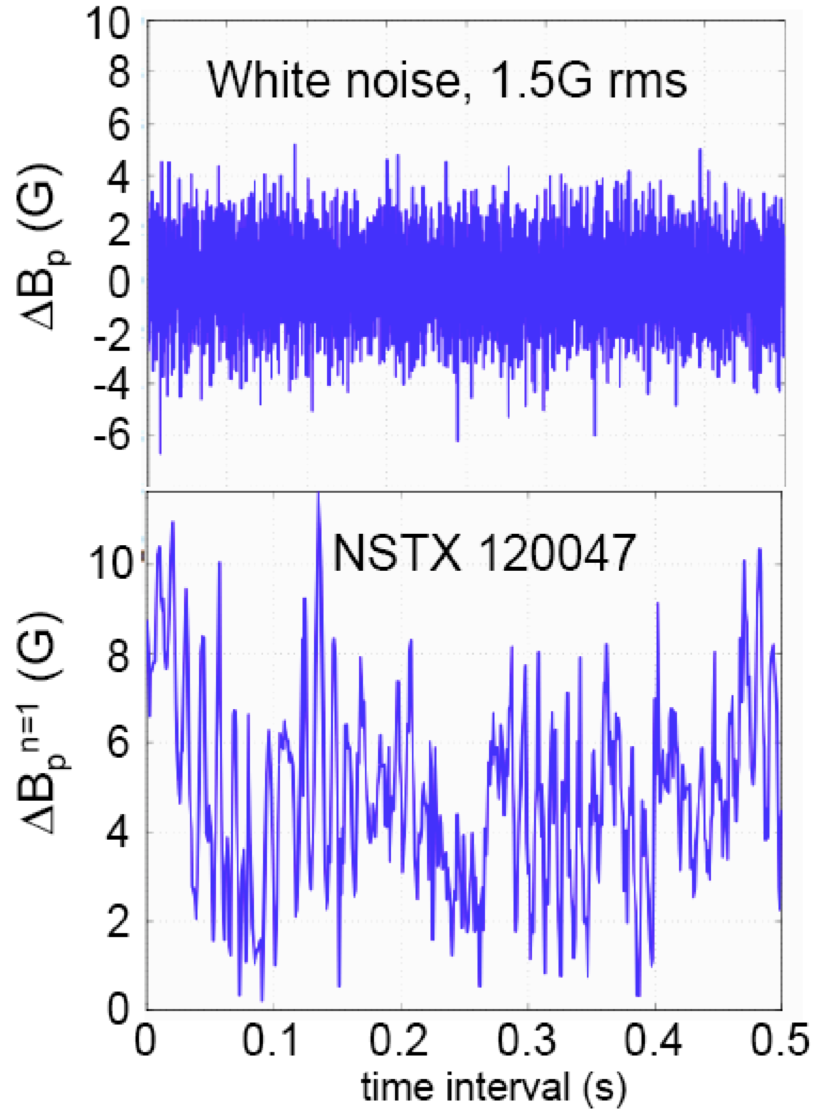

Power estimates bracket needs for KSTAR RWM control

Proportional gain controller

	C_β	White noise (1.6-2.0G RMS) (RMS values) I_{IVCC}(A)	V_{IVCC}(V)	P_{IVCC}(W)	NSTX 120047 ΔB_p sensors (RMS values) I_{IVCC}(A)	V_{IVCC}(V)	P_{IVCC}(W)
Unloaded IVCC: L=10μH, R=0.86mOhm, L/R=12.8ms	80%	30	1.6	45	362	0.7	253
	95%	41	2.0	82	430	0.8	307
FAST IVCC circuit: L=13μH, R=13.2mOhm, L/R=1.0ms	80%	20.9	1.56	30.0	1.9e3	24.9	62e3
	95%	28.3	1.78	50.6	9e3	119	1.8e6

Power estimates bracket needs for KSTAR RWM control

Proportional gain controller / LQG controller

White noise (1.6-2.0G RMS) | NSTX 120047 ΔB_p sensors

	C_β	White noise (RMS values) I_{IVCC}(A)	V_{IVCC}(V)	P_{IVCC}(W)	NSTX 120047 ΔB_p sensors (RMS values) I_{IVCC}(A)	V_{IVCC}(V)	P_{IVCC}(W)
Unloaded IVCC L=10μH R=0.86mOhm L/R=12.8ms	80%	30 / **29**	1.6 / **0.8**	45 / **24**	362	0.7	253
	95%	41 / **35**	2.0 / **0.9**	82 / **34**	430	0.8	307
FAST IVCC circuit L=13μH R=13.2mOhm L/R=1.0ms	80%	20.9	1.56	30.0	1.9e3	24.9	62e3
	95%	28.3	1.78	50.6	9e3	119	1.8e6

- Initial results using advanced Linear Quadratic Gaussian (LQG) controller yield factor of 2 power reduction for white noise.
- LQG controller consists of two steps:
  - Balanced Truncation of VALEN state-space for fixed β_n
  - Optimal controller and observer design based on the reduced order system

Implementation of digital LQG controller

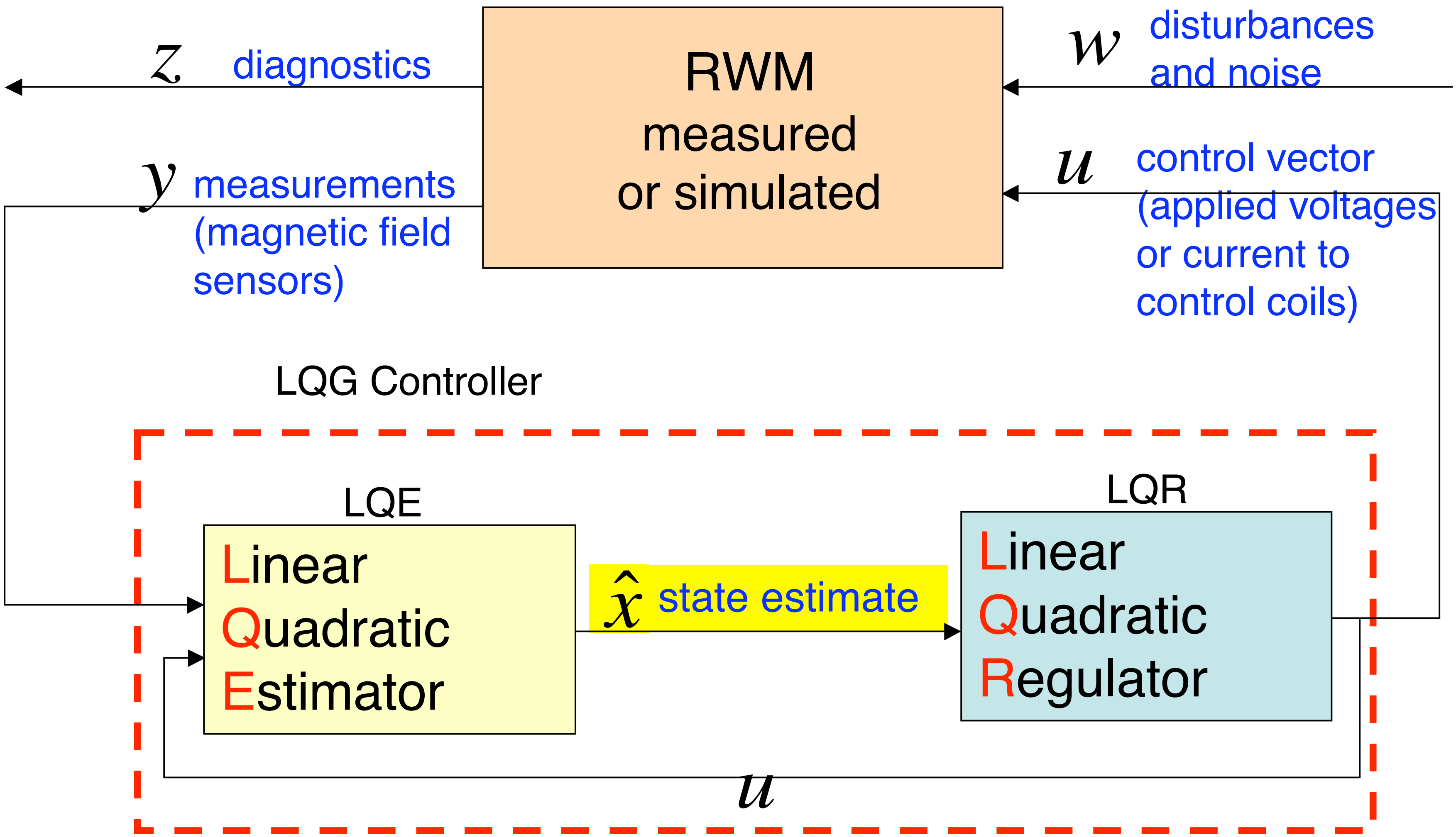

Detailed diagram of digital LQG controller

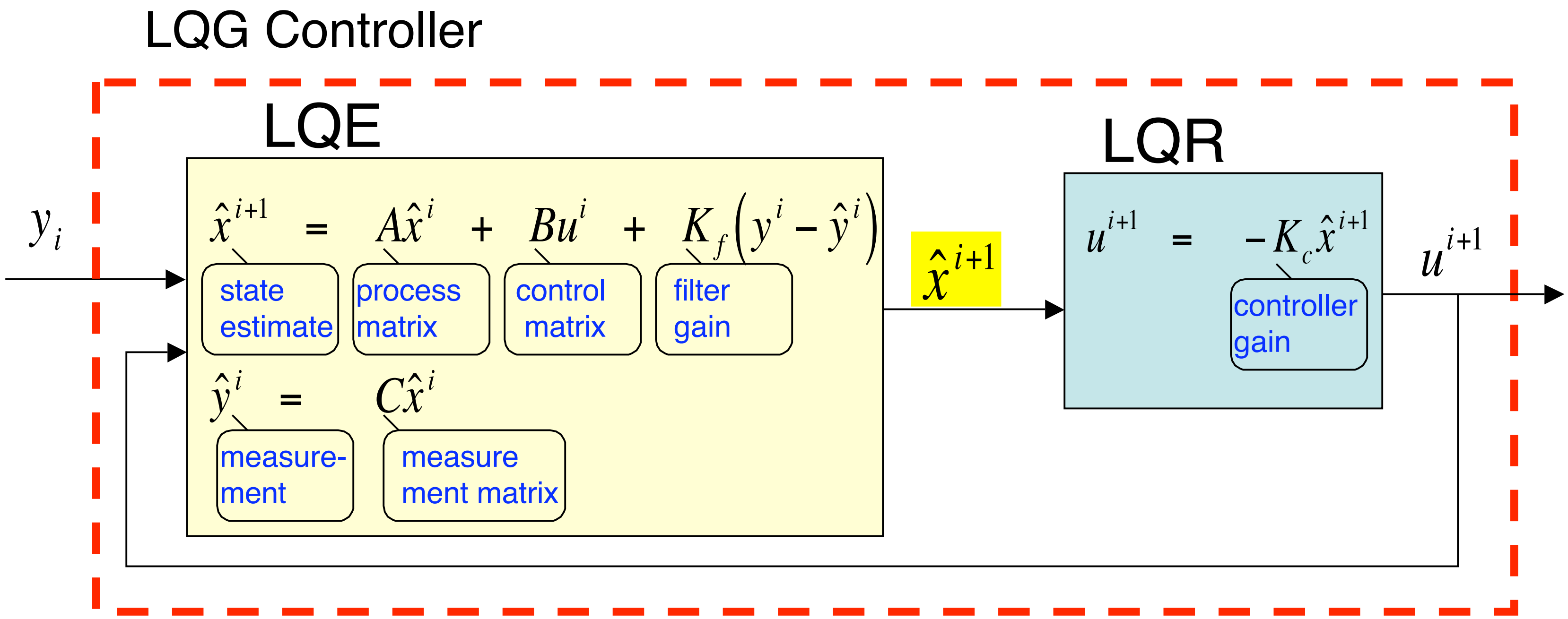

- State estimate stored in LQE provides information about amplitude and phase of RWM and takes into account wall currents
- Dimensions of LQE matrices depends on
  - State estimate (reduced balanced VALEN states)~10-20
  - Number of control coils ~3
  - Number of sensors ~ 12
- All matrixes in LQE and LQR are calculated in advance using VALEN state-space for particular 3-D tokamak geometry

Balanced truncation significantly reduces VALEN state space

Full VALEN computed wall currents:

I

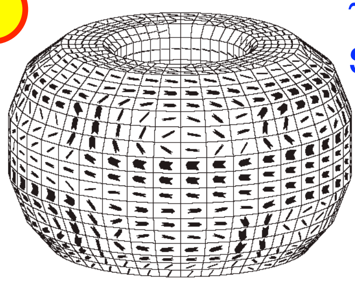

~3000 states

$$\vec{x} = \left(\vec{I}_w \;\; \vec{I}_f \;\; I_d\right)^T; \qquad \vec{u} = \vec{V}_f;$$

$$\overleftrightarrow{A} = -\overleftrightarrow{L}^{-1} \cdot \overleftrightarrow{R}; \qquad \overleftrightarrow{B} = \overleftrightarrow{L}^{-1} \cdot \vec{I}_{cc};$$

$$\vec{y} = \vec{\Phi}; \qquad \overleftrightarrow{C} = \overleftrightarrow{M}$$

sensor fluxes

mutual inductance matrix

Balancing transformation

$$\hat{x} = \overleftrightarrow{T}\vec{x}$$

II

Balanced realization:

RWM fixed phase

$$\left[\begin{array}{c|c} \overleftrightarrow{T}\overleftrightarrow{A}\overleftrightarrow{T}^{-1} & \overleftrightarrow{T}\overleftrightarrow{B} \\ \hline \overleftrightarrow{C}\overleftrightarrow{T}^{-1} & \vec{0} \end{array}\right] = \left[\begin{array}{c|c} \tilde{A} & \tilde{B} \\ \hline \tilde{C} & 0 \end{array}\right] = \left[\begin{array}{cc|c} \tilde{A}_{11} & \tilde{A}_{12} & \tilde{B}_1 \\ \tilde{A}_{21} & \tilde{A}_{22} & \tilde{B}_2 \\ \hline \tilde{C}_1 & \tilde{C}_2 & 0 \end{array}\right]$$

2999 Balanced states:

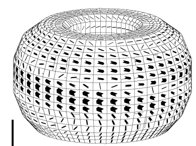

$\hat{x}_1$

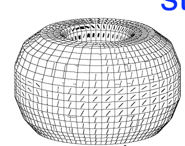

$\hat{x}_2$

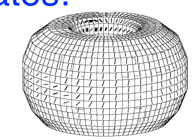

$\hat{x}_3$

...

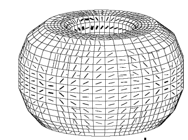

$\hat{x}_{3000}$

Truncation

III **State reduction:**

$$\left[\begin{array}{c|c} \tilde{A}_{11} & \tilde{B}_1 \\ \hline \tilde{C}_1 & 0 \end{array}\right] \equiv \left[\begin{array}{c|c} A & B \\ \hline C & 0 \end{array}\right]$$

~3-20 states

I What is VALEN state-space?

II How to find balancing transformation $\overleftrightarrow{T}$?

III How to determine number of states to keep ?

State-space control approach may allow superior feedback performance

I

- VALEN circuit equations after including plasma stability effects the fluxes at the wall, feedback coils and plasma are given by

$$\vec{\Phi}_w = \overleftrightarrow{\mathrm{L}}_{ww} \cdot \vec{I}_w + \overleftrightarrow{\mathrm{L}}_{wf} \cdot \vec{I}_f + \overleftrightarrow{\mathrm{L}}_{wp} \cdot I_d$$

$$\vec{\Phi}_f = \overleftrightarrow{\mathrm{L}}_{fw} \cdot \vec{I}_w + \overleftrightarrow{\mathrm{L}}_{ff} \cdot \vec{I}_f + \overleftrightarrow{\mathrm{L}}_{fp} \cdot I_d$$

$$\Phi_p = \overleftrightarrow{\mathrm{L}}_{pw} \cdot \vec{I}_w + \overleftrightarrow{\mathrm{L}}_{pf} \cdot \vec{I}_f + \overleftrightarrow{\mathrm{L}}_{pp} \cdot I_d$$

- Equations for system evolution are given by

$$\begin{pmatrix} \overleftrightarrow{\mathcal{L}}_{ww} & \overleftrightarrow{\mathcal{L}}_{wf} & \overleftrightarrow{\mathcal{L}}_{wp} \\ \overleftrightarrow{\mathcal{L}}_{fw} & \overleftrightarrow{\mathcal{L}}_{ff} & \overleftrightarrow{\mathcal{L}}_{fp} \\ \overleftrightarrow{\mathcal{L}}_{pw} & \overleftrightarrow{\mathcal{L}}_{pf} & \overleftrightarrow{\mathcal{L}}_{pp} \end{pmatrix} \cdot \frac{d}{dt} \begin{pmatrix} \vec{I}_w \\ \vec{I}_f \\ I_d \end{pmatrix} = \begin{pmatrix} \overleftrightarrow{R}_w & 0 & 0 \\ 0 & \overleftrightarrow{R}_f & 0 \\ 0 & 0 & \overleftrightarrow{R}_d \end{pmatrix} \cdot \begin{pmatrix} \vec{I}_w \\ \vec{I}_f \\ I_d \end{pmatrix} + \begin{pmatrix} \vec{0} \\ \vec{V}_f \\ 0 \end{pmatrix}$$

- In the state-space form

$$\boxed{\begin{aligned} \dot{\vec{x}} &= \overleftrightarrow{A}\vec{x} + \overleftrightarrow{B}\vec{u} \\ \vec{y} &= C\vec{x} \end{aligned}}$$

where $\vec{x} = \left(\vec{I}_w \;\; \vec{I}_f \;\; I_d\right)^T; \quad \overleftrightarrow{A} = -\overleftrightarrow{\mathrm{L}}^{-1} \cdot \overleftrightarrow{R}; \quad \overleftrightarrow{B} = \overleftrightarrow{\mathrm{L}}^{-1} \cdot \overleftrightarrow{I}_{cc}; \quad \vec{u} = \vec{V}_f$

& measurements $\vec{y} = \vec{\Phi}_s$ are sensor fluxes. State-space dimension ~1000 elements!

- Classical control law with proportional gain defined as $\vec{u} = -\overleftrightarrow{G}_p \vec{y}$

Balanced transformation is determined by controllability and observability grammians

II

- A system $\begin{aligned}\dot{\vec{x}} &= \overleftrightarrow{A}\vec{x} + \overleftrightarrow{B}\vec{u} \\ \vec{y} &= \overleftrightarrow{C}\vec{x}\end{aligned}$ with transfer function: $\left[\begin{array}{c|c} A & B \\ \hline C & 0 \end{array}\right]$

is called controllable if the initial state $\vec{x}(t_0)$ can be steered to any arbitrary state $\vec{x}(t_1)$ in a finite time $(t_1 - t_0)$ by using some control $\vec{u}$.

$$\vec{x}(t_0) \xrightarrow{\vec{u},\quad t\in(t_1 - t_0)} \vec{x}(t_1)$$

is called observable if the initial state $\vec{x}(t_0)$ can be determined uniquely from the output $\vec{y}(t)$ on the range $t\in[t_0,t_1]$

$$\vec{y}(t),\quad t\in[t_0,t_1] \longrightarrow \vec{x}(t_0)$$

KSTAR

Measure of system controllability and observability is given by controllability and observability grammians.

- Given stable Linear Time-Invariant (LTI) Systems $\left[\begin{array}{c|c} A & B \\ \hline C & 0 \end{array}\right]$

- Observability grammian, $\Gamma_o = \int_0^\infty e^{A^T\tau} C^T C e^{A\tau} d\tau$, can be found be solving continuous-time Lyapunov equation, $A^T\Gamma_o + \Gamma_o A + C^T C = 0$, provides measure of output energy:

$$\boxed{\|y\|_2^2 = x_0^T \Gamma_O x_0}$$

- $\Gamma_O = U\Lambda_O U^T$ defines an "observability ellipsoid" in the state space with the longest principal axes along the most observable directions

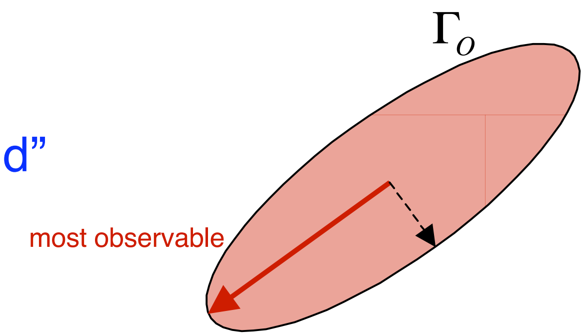

- Controllability grammian, $\Gamma_c = \int_0^\infty e^{A\tau} BB^T e^{A^T\tau} d\tau$, can be found be solving continuous-time Lyapunov equation, $A\Gamma_c + \Gamma_c A^T + BB^T = 0$, provides measure of input(control) energy:

$$\boxed{\|u\|_2^2 = x_0^T \Gamma_C^{-1} x_0}$$

- $\Gamma_C = V\Lambda_C V^T$ defines a "controllability ellipsoid" in the state space with the longest principal axes along the most controllable directions

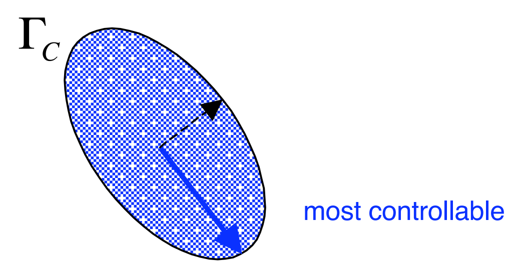

Balanced realization exists for every stable controllable and observable system

II

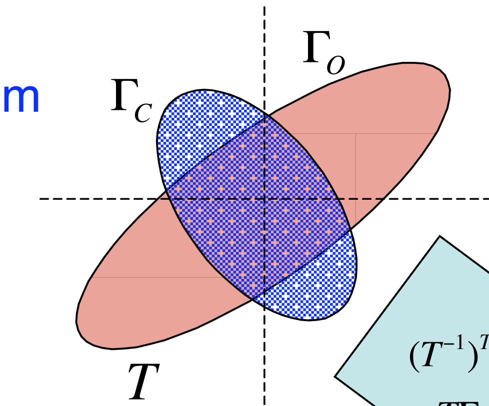

$$\left[\begin{array}{c|c} A & B \\ \hline C & 0 \end{array}\right]$$

- Controllable, observable & stable system called balanced if

$$\tilde{\Gamma}_C = \tilde{\Gamma}_O = \begin{pmatrix} \sigma_1 & 0 & 0 \\ 0 & \ddots & 0 \\ 0 & 0 & \sigma_n \end{pmatrix} = \Sigma,$$

where $\sigma_i > \sigma_j$ for $i > j$

σ_i- Hankel Singular Values

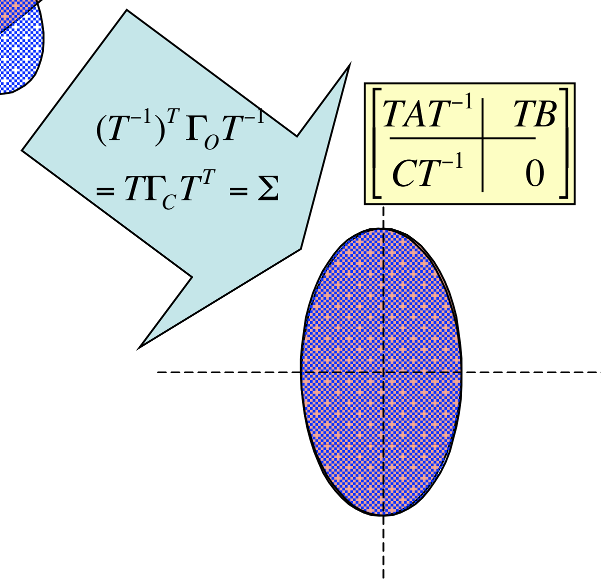

- The balancing similarity transformation transforms the observability and controllability ellipsoids to an identical ellipsoid aligned with the principle axes along the coordinate axes.

- The balanced transformation T can be defined in two steps:
  - Start with SVD of controllability grammian $\Gamma_c = VS_cV^T$
    and define the first transformation as $T_1 := VS_c^{1/2}$
  - Perform SVD of observability grammian in the new basis: $\tilde{\Gamma}_o = T_1^T \Gamma_o T_1 = US_oU^T$
    the second transformation defined as $T_2 := US_o^{-1/4}$
  - The final transformation matrix is given by: $\boxed{T := T_1T_2 = VS_c^{1/2}US_o^{-1/4}}$

HSV spectrum of VALEN state-space analysis suggests the number of modes necessary for the system reduction

III

KSTAR

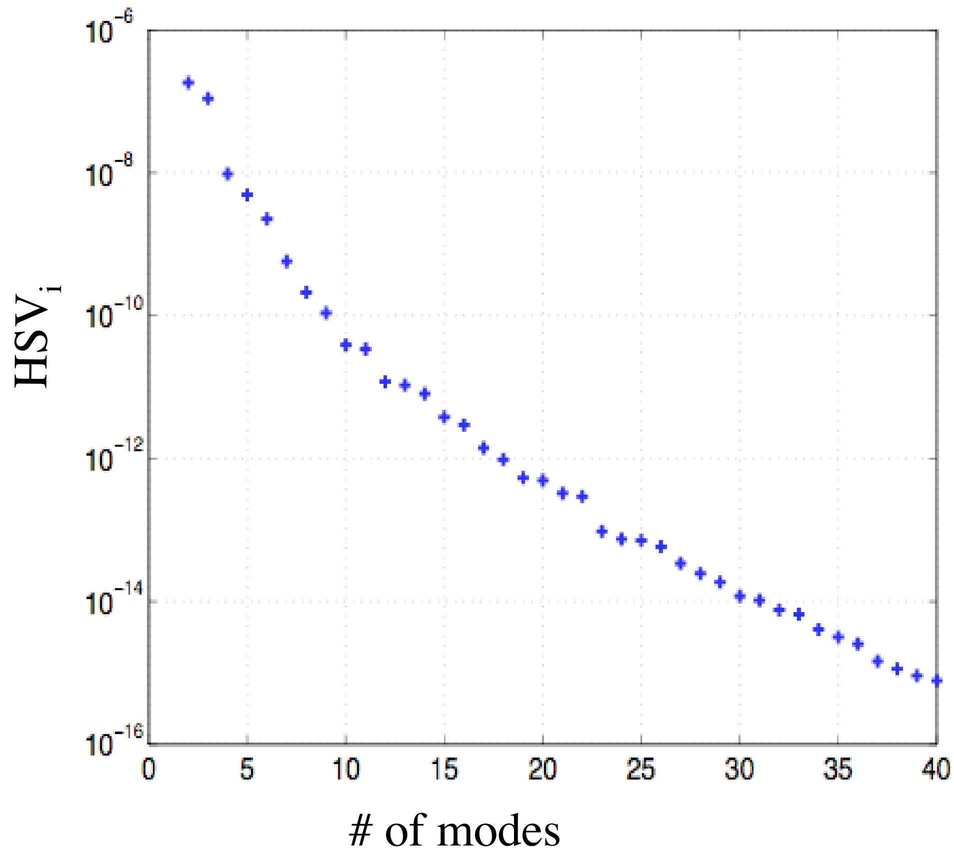

- KSTAR LQG controller uses **4 central IVCC & 16 mid-plane poloidal sensors**
- Clear gaps in KSTAR HSV spectrum
- The number of modes necessary for the system reduction needs to be verified further by actual controller performance designed based on the reduced model

Determination of LQR (optimal controller) gain for the dynamic system

III

For given dynamic process: $\dot{\vec{x}} = \overleftrightarrow{A}\vec{x} + \overleftrightarrow{B}\vec{u}$

Find the matrix $\overleftrightarrow{K}_c$ such that control law $\vec{u} = -\overleftrightarrow{K}_c\vec{x}$

minimizes Performance Index: $J = \int_t^T \left(\hat{\vec{x}}'(\tau) Q_r(\tau) \hat{\vec{x}}(\tau) + \vec{u}'(\tau) R_r(\tau) \vec{u}(\tau) \right) d\tau \to \min$

where tuning parameters are presented by Q_r, R_r - state and control weighting matrixes,

Solution:

Controller gain for the steady-state can be calculated as $K_c = R^{-1} B_r^T S$

Where S is solution of the controller Riccati equation $SA_r + A_r^T S - SB_r R_r^{-1} B_r^T S + Q_r = 0$

Determination of LQE (optimal observer) gain for the dynamic system

III

For given stochastic dynamic process: $\dot{\vec{x}} = \overleftrightarrow{A}_r \vec{x} + \overleftrightarrow{B}_r \vec{u} + \vec{v}$

with measurements: $\vec{y} = \overleftrightarrow{C}_r \vec{x} + \vec{\omega}$

Find the matrix $\overleftrightarrow{K}_f$ such that observer equation $\dot{\hat{x}} = A_r \hat{x} + B_r u + K_f \left(y - C_r \hat{x} \right)$

minimizes error covariance: $E\left\{ (x - \hat{x})(x - \hat{x})^T \middle| y(\tau), \tau \le t \right\} \to \min$

where tuning parameters are presented by $\overleftrightarrow{V}, \overleftrightarrow{W}$ - plant and measurement noise covariance matrix

Solution:

Observer gain for the steady-state can be calculated as $K_f = PC' W^{-1}$

Where P is solution of the observer Riccati equation

$$A_r P + P A_r^T - P C_r^T W^{-1} C_r P + V^T = 0$$

Closed system equations with optimal controller and optimal observer based on reduced order model used for off-line testing

(III)

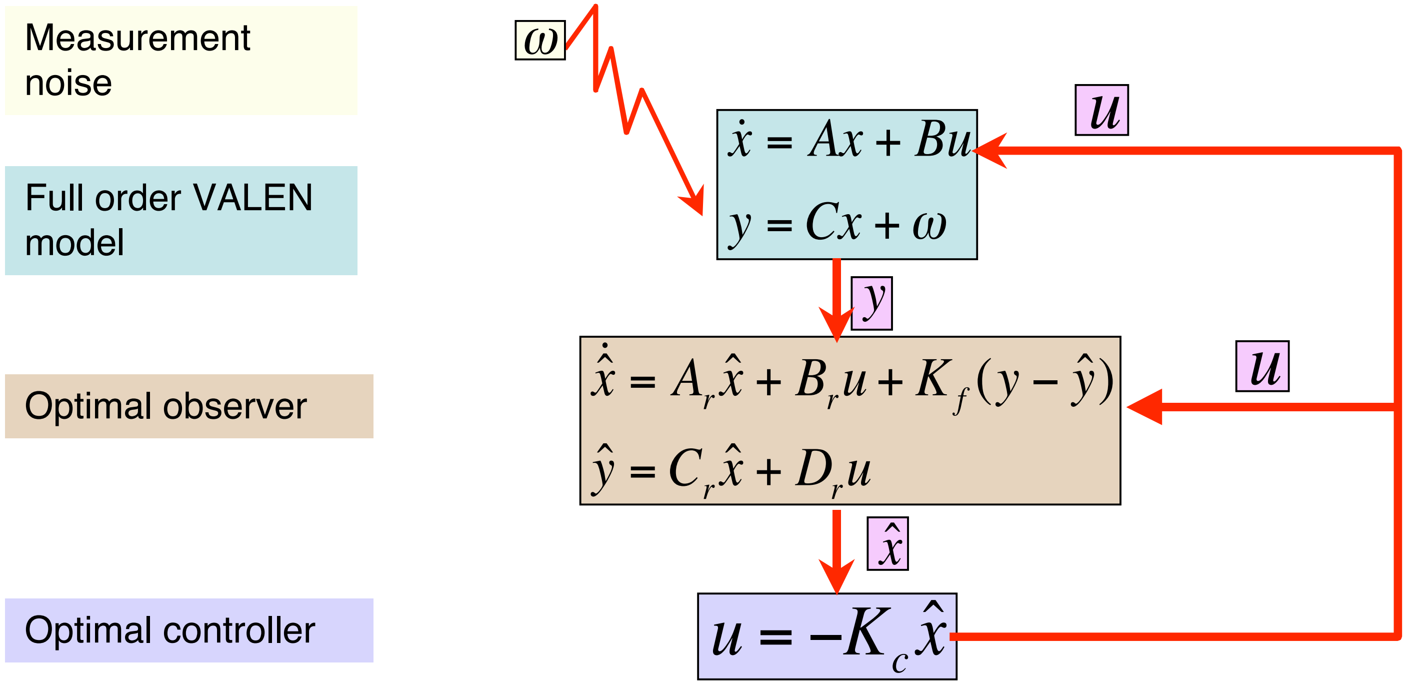

$$\begin{pmatrix} \dot{x} \\ \dot{\hat{x}} \end{pmatrix} = \begin{pmatrix} A & -BK_cC_r \\ K_fC & F \end{pmatrix} \begin{pmatrix} x \\ \hat{x} \end{pmatrix} + \begin{pmatrix} 0 \\ K_f \end{pmatrix} \omega$$

$$F = A_r - K_fC_r - (B_r - K_fD_r)K_cC_r$$

$\Leftarrow$ Closed loop continuous system allows to

- Test if Optimal controller and observer stabilizes original full order model and defined number of states in the LQG controller
- Verify robustness with respect to β_n
- Estimate RMS of steady-state currents, voltages and power

Optimization of observer also reduces number of states needed to stabilize full order unstable system

III

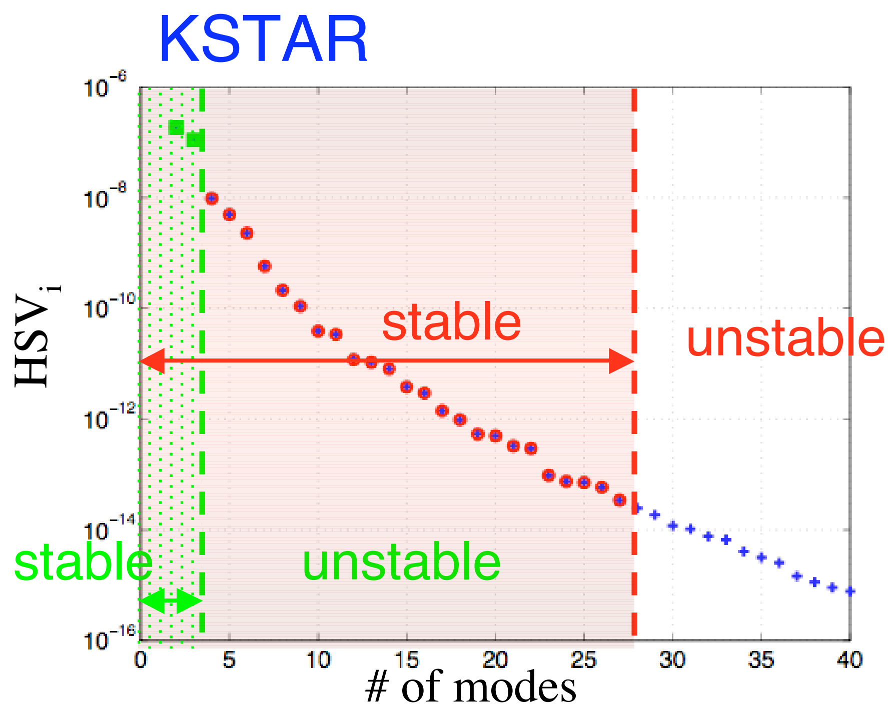

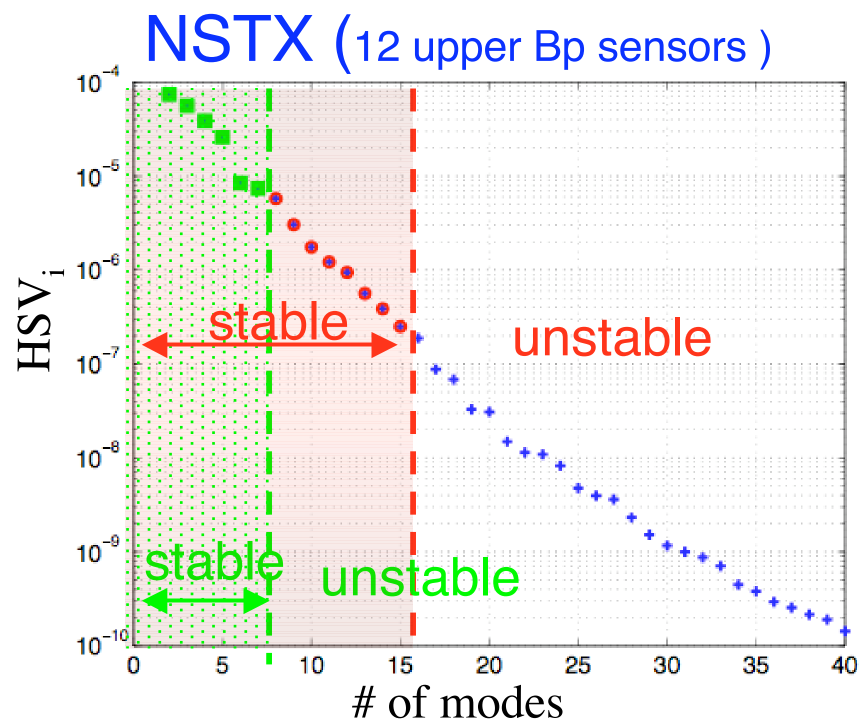

- The first HSV corresponds to unstable RWM and is set to be infinity and not shown on the plots.
- KSTAR state-space based optimal controller and generic observer uses 27 states, and LQG (optimal controller and optimal observer) based on 3 states only.
- NSTX optimal controller and generic observer needs 15 states and LQG (optimal controller and optimal observer) needs only 7 states.

Advanced controller methods planned to be tested on **NSTX** with future application to KSTAR

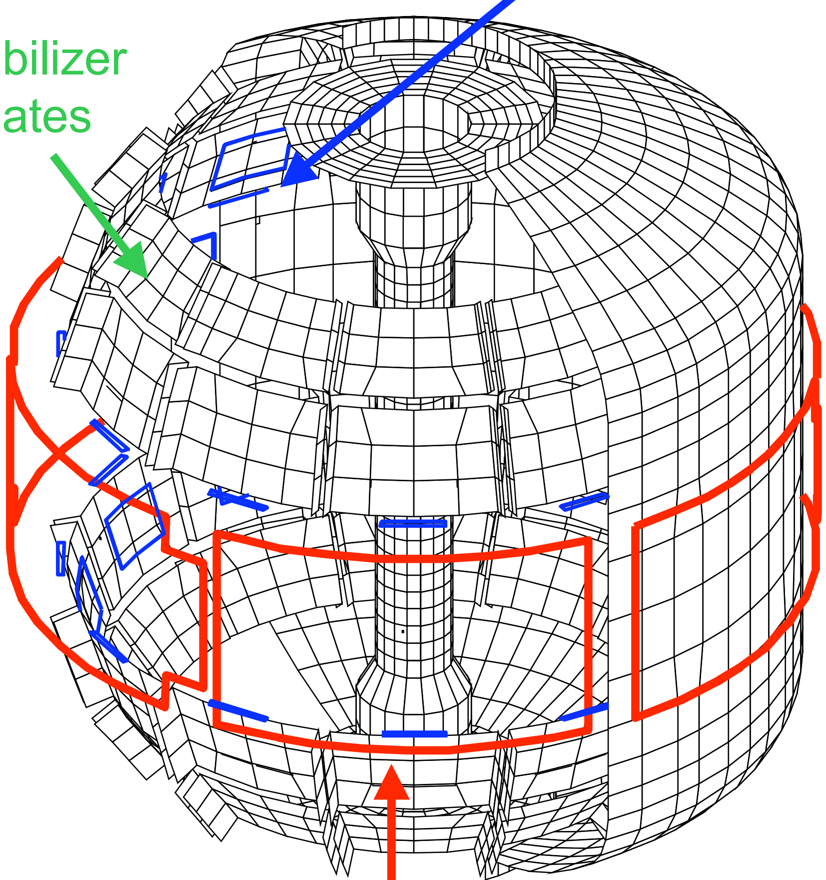

- VALEN NSTX Model includes
  - Stabilizer plates for kink mode stabilization
  - External mid-plane control coils closely coupled to vacuum vessel
  - Upper Bp sensors in actual locations
  - Compensation of control field from sensors
  - Experimental Equilibrium reconstruction (including MSE data)
- Present control system on NSTX uses Proportional Gain

Advanced control techniques suggests significant feedback performance improvement for NSTX up to $\beta_n / \beta_n^{wall} = 95\%$

- Classical proportional feedback methods
  - VALEN modeling of feedback systems agrees with experimental results
  - RWM was stabilized up to β_n = 5.6 in experiment.
- Advanced feedback control may improve feedback performance*
  - Optimized state-space controller can stabilize up to C_β=87% for upper Bp sensors and up to C_β=95% for mid-plane sensors
  - Uses only 15 for optimal controller and generic observer and 7 states for optimal observer and controller design (LQG)

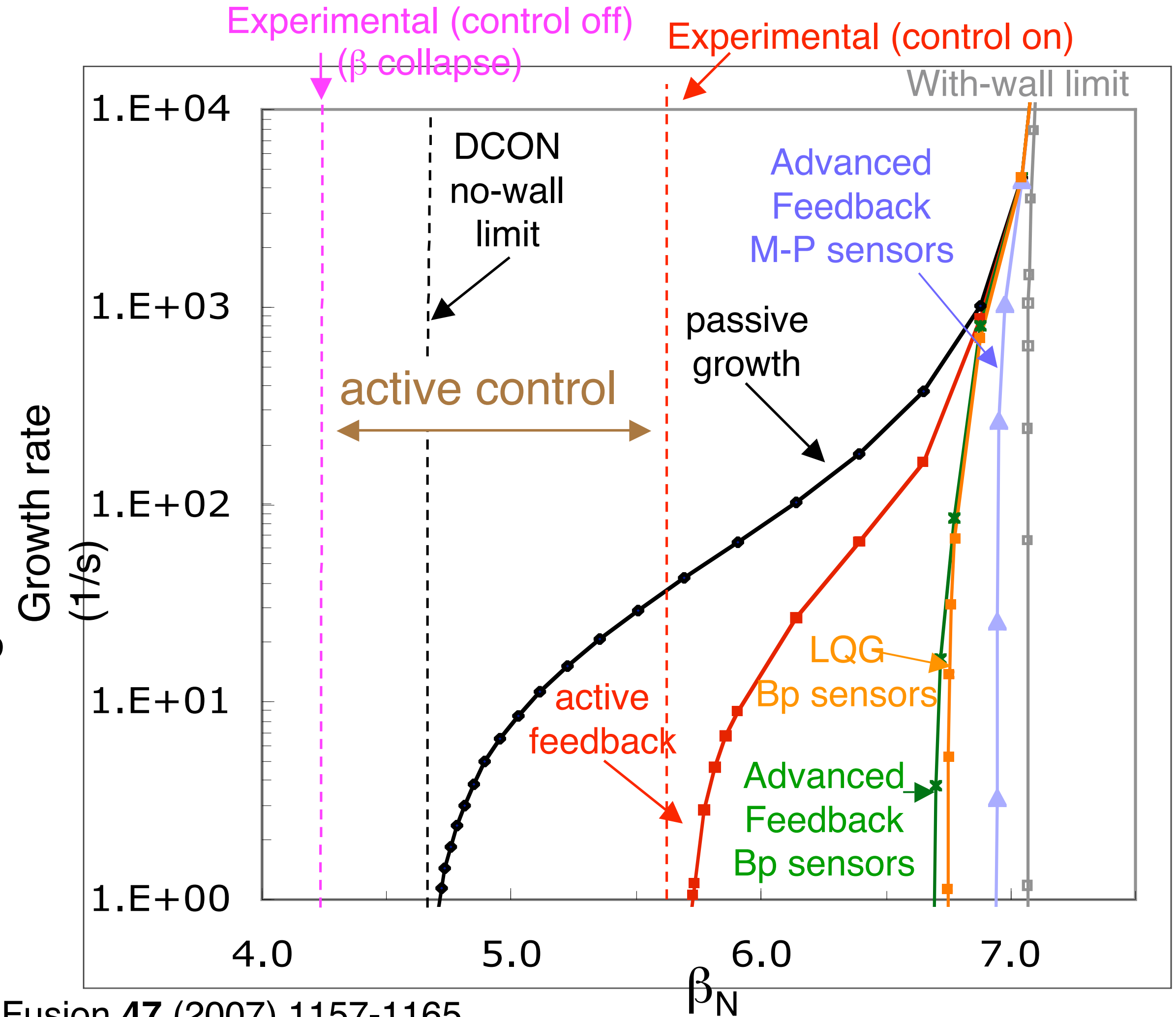

*O.Katsuro-Hopkins at al., Nucl. Fusion **47** (2007) 1157-1165.

Using existing experimental data LQE can be tested off-line

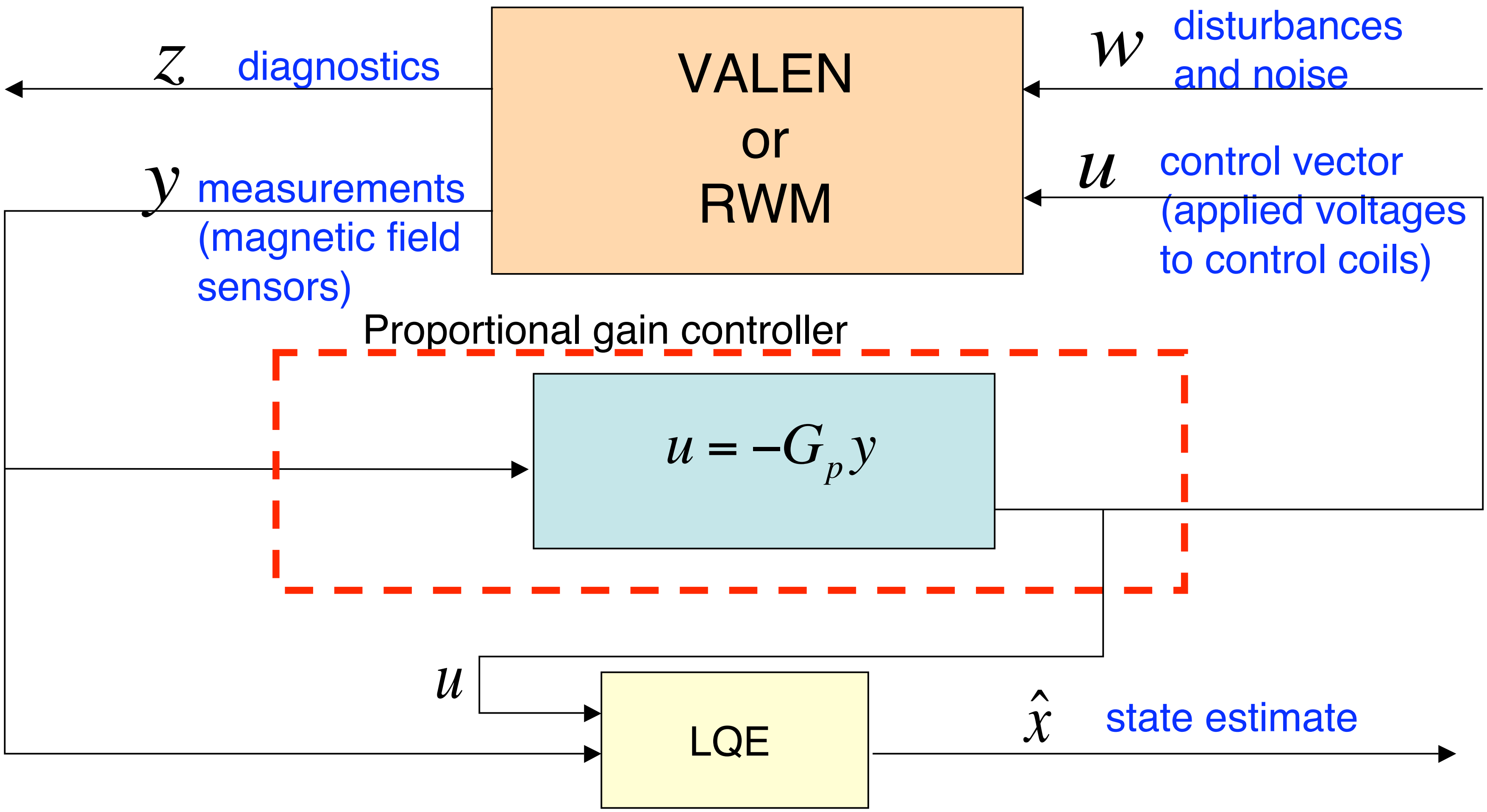

- State estimate $\hat{x}$, calculated in observer provides information about the phase and amplitude of the RWM and can be compared with diagnostic z

At least three ways to stabilize RWM with varying phase

- LQG can be designed based on VALEN with rotating mode, represented by sine and cosine terms (gives phase information).
- Phase can be identified using existing Fourier decomposition tools and consequent application of a look up table for LQG parameters precalculated for fixed mode phases of non-rotating mode.
- RWM phase can be determined using the sensor measurements and geometry and implemented in the reduced VALEN state-space form.

Next steps and future work on the KSTAR stability analysis

- Expand equilibrium / ideal stability analysis as needed
  - Collaborate on equilibrium reconstructions of first plasmas
- Closer definition of RWM control system circuit by interaction with KSTAR engineering team
- Improved noise model for KSTAR sensor noise
- LQG controller with plasma rotation for KSTAR
- LQG controller tests on NSTX with application to KSTAR RWM control system design
- Critical latency testing for KSTAR RWM control

KSTAR is capable of producing long-pulse, high β_n stability research

- Machine designed to run high β_n plasmas with low l_i and significant plasma shaping capability
- Large wall-stabilized region to kink/ballooning modes with $\beta_n / \beta_n^{no\text{-}wall} = 2$ at highest β_n predicted for the device
  - Co-directed NBI, passive stabilizers allow kink stabilization
- Active IVCC mode control system provide effective RWM control
  - IVCC design allows active $n = 1$ RWM stabilization at very high $C_\beta > 98\%$
- Fast IVCC circuit for stabilization is possible at reasonable power levels